



Structural stability of coprecipitated natural organic matter and ferric iron under reducing conditions

Yumiko K. Henneberry^a, Tamara E.C. Kraus^b, Peter S. Nico^{c,*}, William R. Horwath^a

^a Department of Land, Air and Water Resources, University of California, Davis, One Shields Ave., CA 95616, USA

^b US Geological Survey, California Water Science Center, 6000 J. Street, Placer Hall, Sacramento, CA 95819, USA

^c Earth Sciences Division, Lawrence Berkeley National Laboratory, 1 Cyclotron Road, Berkeley, CA 94720, USA

ARTICLE INFO

Article history:

Received 17 September 2011

Received in revised form 28 March 2012

Accepted 23 April 2012

Available online 30 April 2012

ABSTRACT

The objective was to assess the interaction of Fe coprecipitated with dissolved organic matter (DOM) and its effect on Fe (hydr)oxide crystallinity and DOM retention under abiotic reducing conditions. A Fe-based coagulant was reacted with DOM from an agricultural drain and the resulting precipitate (floc) was exposed to S(-II) and Fe(II). Solution concentrations of Fe(II/III) and DOM were monitored, floc crystallinity was determined using X-ray diffraction, and the composition and distribution of functional groups were assessed using scanning transmission X-ray microscopy (STXM) and near edge X-ray absorption fine structure (NEXAFS) spectroscopy. Results indicate coprecipitation of Fe(III) with DOM forms a non-crystalline floc that withstands crystallization regardless of change in pH, Fe:DOM ratio and type of reductant added. There was no evidence that exposure to reducing conditions led to release of DOM from the floc, indicating that coprecipitation with complex natural DOM in aquatic environments may stabilize Fe (hydr)oxides against crystallization upon reaction with reduced species and lead to long term sequestration of the DOM. STXM analysis identified spatially distinct regions with remarkable functional group purity, contrary to the model of DOM as a relatively uniform complex polymer lacking identifiable organic compounds. Polysaccharide-like OM was strongly and directly correlated with the presence of Fe but showed different Fe binding strength depending on the presence of carboxylic acid functional groups, whereas amide and aromatic functional groups were inversely correlated with Fe content.

© 2012 Elsevier Ltd. All rights reserved.

1. Introduction

The coprecipitation of Fe and dissolved organic matter (DOM) is common in soil, sediments, surface water and subsurface aquifers, systems that experience significant variation in either redox or pH conditions (Fuller et al., 1993; Pokrovsky and Schott, 2002). These interactions are hypothesized to play a role in immobilizing DOM and stabilizing it against microbial degradation, as well as controlling the structure and reactivity of natural Fe (hydr)oxides (von Luetzow et al., 2006; Eusterhues et al., 2008). Thus, OM–Fe coprecipitates represent an important class of structures whose chemistry and reactivity require further understanding under different environmental conditions since Fe speciation and mobility affect the availability, cycling, and transport of metals, OM and nutrients.

Coprecipitation of Fe and DOM can occur where reduced water (e.g. lake sediments, mine drainage water, aquifers) comes into contact with oxidized water, causing soluble Fe(II) to be transformed to relatively insoluble Fe(III), which concurrently sorbs ions

and compounds such as metals and OM (Fuller et al., 1993). In estuarine environments, coprecipitation of OM and Fe oxides occurs where salinity causes an increase in the ionic strength of incoming freshwater and subsequent precipitation (Sholkovitz, 1976). Similar phenomena occur in saturated soil exposed to air, such as in wetlands.

In a process that mimics natural coprecipitation of Fe and DOM, the water treatment industry frequently uses Fe-based salts to remove DOM from water prior to disinfection (Dempsey et al., 1984; Siélichi et al., 2008). The technique is used to prevent formation of carcinogenic halogenated byproducts (e.g. chloroform) during disinfection, which result from reaction of chlorine with DOM. The resulting precipitate is an organo-Fe complex, commonly termed “floc.” While the floc resulting from coagulation in water treatment is typically disposed of in landfills, there are cases where reservoirs or constructed wetlands are used as settling ponds to retain the residual floc (Bachand et al., 2000, 2006; Downing et al., 2008). The use of on-site coagulation to remove DOM and improve agricultural drainage water quality is underway in the Sacramento-San Joaquin Delta (Mourad, 2003; Henneberry et al., 2011). Accumulation of the resulting floc in constructed wetlands is intended to help reverse land subsidence in the region. One of the main

* Corresponding author. Tel.: +1 510 486 7118; fax: +1 510 486 5686.

E-mail address: psnico@lbl.gov (P.S. Nico).

uncertainties regarding both natural and synthetic Fe–DOM complexes is their stability under changing environmental conditions. For example, if small changes in pH or redox conditions cause significant re-release of DOM, then the ability of the method to immobilize and stabilize DOM over the long term would be greatly diminished.

Studies of DOM Fe (hydr)oxide structures have found greater structural disorder in the coprecipitated Fe phases vs. organic-free or synthetic ferrihydrite (Eusterhues et al., 2008; Mikutta et al., 2008; Cismasu et al., 2011; Mikutta, 2011). The implications of these structural changes on biogeochemical processes remain unresolved. Under low DOM or DOM-free conditions, poorly crystalline Fe (hydr)oxides like ferrihydrite are highly reactive and a dominant adsorbent of metals and nutrients in aquatic and terrestrial systems, even at low Fe concentration (Larsen and Postma, 2001; Hiemstra and Van Riemsdijk, 2009). However, these poorly crystallized minerals have also been found to be highly susceptible to microbial reduction and dissolution in both soil and aquatic environments (Glasauer et al., 2003; Weiss et al., 2004). They may thus recrystallize into more ordered, lower surface area Fe minerals, such as goethite or magnetite, with subsequent decrease in reductive potential and sorptive capacity.

The presence of various ions and electron donors in solution has been found to both catalyze and inhibit the crystallization of ferrihydrite (Wehrli et al., 1989). Fe(II), formed either abiotically or via Fe reducing microorganisms, has been found to catalyze the transformation of ferrihydrite into more crystalline materials such as goethite and magnetite (Benner et al., 2002; Tufano et al., 2009). However, only a few studies have investigated the effect of OM on the reactivity of poorly crystalline ferric (hydr)oxides under reducing conditions. In these studies, OM has been found to both enhance and inhibit crystallization of ferrihydrite under aerobic and anaerobic conditions (Cornell and Schwertmann, 1979; Cornell and Schneider, 1989; O'Loughlin et al., 2010). Most of the studies used simple or synthesized organic compounds such as citric and tartaric acids and oxalate rather than more complex, naturally occurring OM. As DOM is composed of a diverse array of components, there is a need to determine the effect that coprecipitation with natural, structurally heterogeneous OM has on Fe reactivity. In addition, studies that focus on the effect of multiple reducing agents on Fe–mineral reduction are lacking. Such knowledge is important in order to predict the fate of poorly crystalline iron (hydr)oxides in environments such as wetlands that experience fluctuating pH and redox conditions.

The two primary objectives of this study were to (i) determine the impact of DOM on the propensity of poorly crystalline Fe (hydr)oxide to recrystallize into more stable lower surface area phases and (ii) determine floc stability, defined as the ability to retain OM under reducing conditions. Reducing conditions were simulated by addition of Fe(II) or S(-II). Scanning transmission X-ray microscopy (STXM) was used to examine Fe–OM interactions, and X-ray diffraction (XRD) to monitor changes in floc crystallinity, and solution characteristics to assess DOM and Fe release over time.

2. Materials and methods

2.1. Incubation experiments

Water samples were collected on September 15, 2010 from an agricultural drain on Twitchell Island receiving rice field effluent. Twitchell Island is on the western portion of the San Francisco Bay Delta (California, USA). In the late 1800s the island, formerly a wetland, was drained for agricultural purposes. Current land use on the island includes rice farming, livestock pasture, corn, alfalfa and constructed wetlands. Dissolved organic carbon (DOC) concen-

tration in the drainage water typically ranges between 0.5 and 7.5 mmol l⁻¹ (6–90 mg l⁻¹) (Deverel et al., 2007; Kraus et al., 2008). Soil on the island is Rindge mucky silt loam (Euic, thermic Typic Haplosaprist), formed from Tule and reed deposition (Tugel, 1993).

A sample of agricultural drainage water was collected using an Amazon submersible pump and high purity, plasticizer-free 1.27 cm Tygon tubing. The water was filtered directly in the field through a 0.2 µm in-line membrane filter (General Electric Memtrex, 25.4 cm). Samples were directly transferred to a clean 19 l Al ball lock soda keg. Water was stored in the dark at 4 °C for ca. 2 weeks prior to experimental procedures and analysis.

As the water may have reached anoxic conditions due to the combination of high daytime temperature and stagnant water conditions within the drain, the sample was purged with O₂ (2 h) prior to experimentation to ensure that DOM and Fe concentration would resemble that of aerated flowing water typically found in the drains. After oxidation, water was passed through 0.3 µm ashed, quartz fiber filters.

A coagulant solution (1.75 M) was made by mixing Fe₂(SO₄)₃ powder in reagent grade 9 M H₂SO₄. The amount of coagulant required to remove the maximum amount of DOC was determined using a streaming current detector (SCD), a common method used by water utilities to determine coagulant dosing requirements. The SCD measures the electrical charge on colloids in water and is an indicator of the extent of destabilization (Dentel and Kingery, 1989). Optimal dose is reached when the SCD indicates a neutral solution. The amount of C and Fe in the floc was calculated as the difference between the concentration in solution prior to and following coagulation (after filtration through a 0.2 µm membrane). The ratio of DOC in solution to Fe added as coagulant was varied, resulting in 47–78% DOC removal and floc molar C:Fe values from 1.9 to 3.5, representing maximum DOC removal conditions to lesser values, respectively (Table 1).

Coagulation of solutions varying in initial C:Fe values was conducted using a six paddle mixer (Phipps and Bird 900, Richmond, VA, USA) at 250 rpm for 3 min and 40 rpm for 15 min. Final pH was adjusted to 6.5 ± 0.1 with 5 M NaOH. The solutions were left (1 h) to allow flocculation to be complete. Aliquots (50 ml) were transferred from the batch solutions, with stirring (magnetic bar), to 50 ml crimp-top glass serum vials with rubber butyl septa and Al rings.

In an unbuffered system, the addition of Fe(II) and S(-II) results in a decrease and increase in pH, respectively. To remove the effect of pH, which could potentially confound crystallization (Schwertmann and Murad, 1983), we added PIPES (1,4-piperazinediethane sulfonic acid) buffer to maintain a system at 6.5 pH. The PIPES buffer was chosen because it does not react with Fe species; however, it is a concentrated organic compound and thus masks change in DOC concentration in the system. We therefore conducted two experiments: (i) an unbuffered system, in which floc C:Fe ranged from 1.9–2.4 and (ii) a buffered system with floc C:Fe between 2.5 and 3.5 (Table 1). In the unbuffered system, the samples were pipetted as above into serum vials. In the buffered system, PIPES was added after the addition of NaOH, to a final concentration of 7 mM.

All sample preparation and extractions were conducted in an anaerobic glove box maintained under a N₂ atmosphere (specialty grade, 99.9%). Samples were sparged with N₂ (15 min) before being transferred to the anaerobic chamber.

The effect of two different reductants, Fe(II) and sulfide S(-II), on floc crystallinity was tested. Fe(II) was added by injecting a concentrated stock solution (0.001 M or 1 M) of FeSO₄ to a final concentration between 0.01 mM and 3.97 mM (Table 1). S(-II) was added via injection of a stock solution of Na₂S (0.01 M or 0.1 M) to a solution concentration range of 0.05–0.6 mM. Concentration values of the

Table 1
Initial treatment solution conditions.

Treatment	Fe(III) added as coagulant (mmol l ⁻¹)	DOC removed (%)	C:Fe in floc (mol:mol) ^a	Fe(II) added as reductant (mmol l ⁻¹)	S(II) added as reductant (mmol l ⁻¹)
<i>Unbuffered treatments</i>					
Unbuffered, higher concentration of coagulant added	3.7	78	1.9	Low: 0.01 High: 3.5	Low: 0.05 High: 0.6
Unbuffered, lower concentration of coagulant added	2.2	55	2.4	Low: 0.01 High: 2.5	Low: 0.05 High: 0.6
<i>Buffered treatments</i>					
Buffered, higher concentration of coagulant added	2.2	55	2.5	Low: 0.01 High: 3.8	Low: 0.05 High: 0.6
Buffered, lower concentration of coagulant added	1.3	47	3.5	Low: 0.01 High: 2.3	Low: 0.05 High: 0.6

^a Ratio of initial floc prior to reductant addition.

Fe(II) were selected to mimic those in natural wetlands (below detection to 300 μM; Blodau et al., 2002; Emerson and Weiss, 2004; Knorr et al., 2009) to values resulting in an Fe(II):Fe(III) of 1–1.8. S(-II) concentrations were selected to cover the range of values for wetlands (0–6.2 mM; Blodau et al., 2002; Choi et al., 2006).

To determine whether the presence of DOM affected floc re-crystallization, all reducing treatments were also applied to vials containing coagulant added to DI water with no DOM. To ensure crystallization of Fe did not occur in the absence of reductant, samples (both with and without OM), that did not receive reductant, were also examined.

Treatments were conducted in triplicate except for the buffered treatment with a higher ratio of C:Fe (3.5; Table 1), which was not replicated. All samples were destructively sampled on days 0 (2–3 h following initial preparation), 5 and 14.

2.2. Solution analysis

DOC concentration was determined by UV-persulfate digestion (Teledyne-Tekmar Phoenix 8000). The absorption at 254 nm was measured on filtered samples at constant temperature (25 °C) with a Cary 300 spectrophotometer using a 1 cm quartz cell and distilled water as blank. To eliminate interference from Fe(III) in absorbance (UV) measurements, 0.05 ml 5% hydroxylamine hydrochloride was added to 1 ml sample and absorbance data recorded until no further change, indicating that all the Fe(III) had been reduced to non-interfering Fe(II), a process that takes ca. 10 min (Doane and Horwath, 2010). Specific UV absorbance (SUVA), a proxy for aromaticity, was calculated by dividing absorbance at 254 nm by DOC concentration, and is reported in l mg C⁻¹ m⁻¹ (Weishaar et al., 2003). Total dissolved Fe, Fe(II) and Fe(III) were determined colorimetrically with ferrozine (Viollier et al., 2000; Pullin and Cabaniss, 2001). One way ANOVA was used to determine significant differences between DOC concentration and SUVA values using the R statistical program (version 2.10.1). Initial water quality characteristics can be found in Table 2.

2.3. Floc analysis

2.3.1. STXM

The detailed C and Fe associations in fresh aerated sample floc material were investigated using STXM in conjunction with near edge X-ray fine structure (NEXAFS) spectroscopy at beamline 5.3.2.2 of the Advanced Light Source Facility in Berkeley, California (Warwick et al., 2002). Samples were prepared by pipetting small aliquots of freshly prepared floc onto a 100 nm thick Si₃N₄ membrane, followed by transfer to the sample chamber maintained under a He atmosphere. Carbon NEXAFS spectra were collected from 280 eV to 330 eV and Fe spectra from 700 to 730 eV. Functional

Table 2
Initial water quality characteristics of rice drain water.

DOC (mmol l ⁻¹)	pH	EC (μS cm ⁻¹) ^a	SUVA (l mg ⁻¹ cm ⁻¹)	FeT (mmol l ⁻¹) ^b
9.7	8.4	2.2	3.1	7.1 × 10 ⁻³

^a Electrical conductivity.

^b Total dissolved iron.

group distribution images were calculated by subtracting pairs of images, one from below the C adsorption edge at 284.3 eV and the others from energies associated with peak absorbance, for the desired functional groups, viz. aromatic (285.5 eV), amide (288.3 eV), carboxylic (288.7 eV). The aXIS family of programs was used to extract spatially resolved spectra. Although five stacks of data were collected, only three had adequate quality for detailed analysis.

2.3.2. XRD

After the set incubation time, floc samples were transferred to vials, capped and centrifuged at 2.3 × 10³ rcf (15 min). The vials were returned to the glove box, the solution was decanted and the remaining floc was pipetted onto clean glass slides and dried under N₂. To prevent oxygenation, the slides were sealed with Kapton tape. A similar set-up using titanium citrate solution as a color indicator indicated the Kapton tape maintained anoxic conditions for >8 h. Samples were scanned immediately upon removal from the glove box. From each treatment, one replicate was scanned.

X-ray diffraction scans were performed with a Rigaku Ultima IV horizontal goniometer (Rigaku Corp., Japan) using Cu Kα radiation at 40 kV and 40 mA, step scanning from 2° to 60° 2θ at increments of 0.02° 2θ. Baseline subtraction and data processing were conducted with JADE (v 9.0.2, Materials Data, Inc., Livermore, CA). To clearly differentiate mineral peaks from the background noise, a limit of detection line was calculated as the 97.5% confidence interval around the angle-dependent mean of a time zero diffractogram of Twitchell DOM coagulated at 100%.

3. Results and discussion

3.1. STXM characterization of fresh floc material

The use of STXM provides spatially resolved elemental and chemical information for a sample not under high vacuum conditions, making it an ideal tool for floc analysis. The distributions of C and Fe in three separate flocs were identified; two are shown in Fig. 1. In general, C was highly spatially correlated with Fe in both floc particles, with the exception of Regions 1 and 2, which show no detectable Fe concentration (Fig. 1a). Fig. 1c shows the relative distribution of OM functional groups for the particle depicted in Fig. 1a, with aromatic rich OM in red (285.5 eV), amide rich OM in

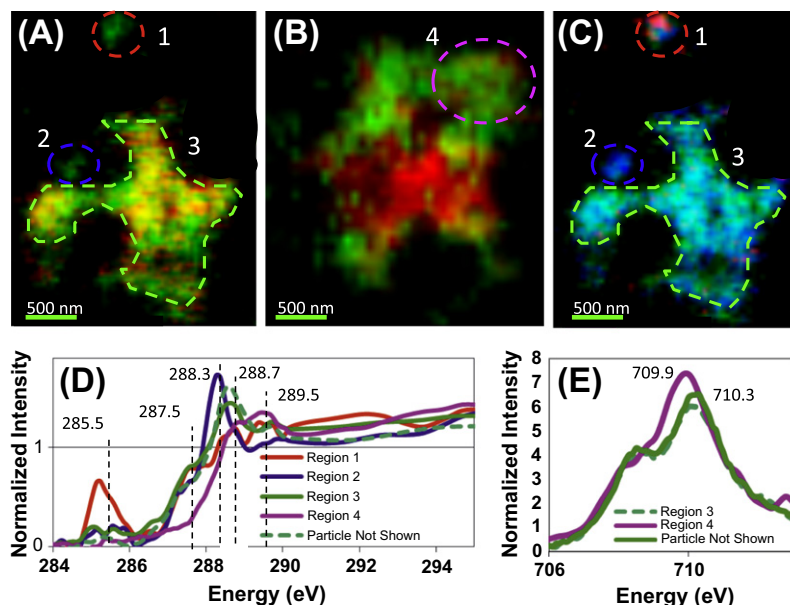


Fig. 1. (A and B) STXM images depicting C and Fe distribution on two different floc particles; green, carbon distribution; red, iron distribution. (C) Distribution of functional groups on floc shown in (A); red, aromatic rich; blue, amide rich; green, carboxylic rich. (D and E) NEXAFS spectra of corresponding regions of floc in (A–C). (For interpretation of the references to color in this figure legend, the reader is referred to the web version of this article.)

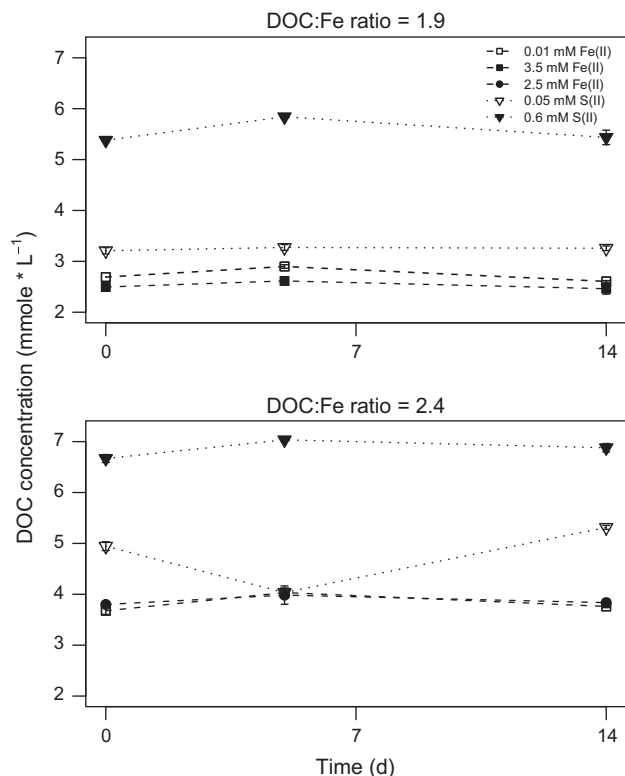


Fig. 2. DOC concentration in solution for two unbuffered solutions with OM receiving different concentrations of reductant. Top panel depicts treatment with higher Fe coagulant dose (3.7 mM), while bottom panel represents treatment with lower Fe coagulant dose (2.2 mM). DOC: Fe ratio is for values within the floc. Points depict mean, vertical lines show standard deviation of the mean ($n = 3$).

blue (288.3 eV) and carboxylic rich OM in green (288.7 eV). The functional group distribution for the particle in Fig. 2b was more uniform and the image shown represents the intensity at O-alkyl material (289.5 eV) (Christl and Kretzschmar, 2007; Chan et al., 2009). Interestingly, in Fig. 1a the OM associated with the Fe mate-

rial is carboxyl rich, while both the amide and aromatic rich areas are inversely correlated with Fe content (Fig. 1a and c).

Corresponding NEXAFS spectra for the floc particles were also collected for C and Fe. The shape of the spectra is sensitive to the composition of the corresponding material. The C spectrum associated with Region 1 (Fig. 1d) shows a large peak at 285.5 eV assigned as aromatic C, while the Region 2 spectrum has, as the major feature, a peak at 288.3 eV associated with amide functionality (Cismasu et al., 2011). The Region 3 spectrum, which comprises the bulk of the floc, as well as the spectrum from a third floc particle (not shown), is dominated by the 288.7 eV feature, indicating a large fraction of carboxyl groups, and a shoulder at ca. 287.5 eV associated with polyvalent metal complexation of carboxyl groups (Armbruster et al., 2009). The Region 4 spectrum is dominated by a 289.5 eV feature associated with O-alkyl material and consistent with non-carboxyl containing polysaccharides (Christl and Kretzschmar, 2007; Chan et al., 2009). Comparison of the Fe NEXAFS spectra from Regions 3 and 4 shows a distinct shoulder at 708.5 in Region 3 spectra, largely absent from the Region 4 spectra (Fig. 1e). In addition, the position of the dominant peak shifts to slightly lower energy from Region 3 to Region 4, 710.3 to 709.9 respectively. Another particle, not shown, exhibits similar C and Fe NEXAFS spectra to that of Region 3. The primary inference to be made from the differences in the Fe NEXAFS is that Fe spectral shape appears to correlate with the functional group characteristics of the associated C. This implies that the majority of Fe atoms in the floc are directly associated with C functional groups, in contrast to a conceptual model in which the OM is only associated with the surface of a Fe mineral phase. The specific shape of the Fe NEXAFS spectra is determined by three factors: electrostatic multiplet effects, ligand field effects and degree of bonding covalency (Hocking et al., 2010). The less distinct shoulder at 708.5 eV in the Region 3 spectra implies that the Fe–OM complexes in this floc have either lower crystal field stabilization or greater orbital covalency.

The highly distinct nature of the individual C NEXAFS spectra (Fig. 1d) contrasts with the remarkable similarity of C NEXAFS spectra of bulk DOM reported by Schumacher et al. (2006) and Christl and Kretzschmar (2007). This emphasizes that, while bulk

Table 3

Iron concentration and pH upon addition of reductants (Y, yes; N, no; s.d., standard deviation; n.d., no detection; data for samples with no DOM can be found in the Supplementary Table).

DOC: Fe	Reductant	Reductant added (mmol l ⁻¹)	Day	Buffer added	Fe(II) (mmol l ⁻¹)	s.d.	Fe(III) (mmol l ⁻¹)	s.d.	pH	s.d.
1.9	Fe(II)	0.01	0	N	nd	–	nd	–	6.8	0
1.9	Fe(II)	0.01	5	N	3.77E–04	1.45E–04	1.84E–03	1.95E–04	6.6	0.1
1.9	Fe(II)	0.01	14	N	3.77E–04	5.86E–05	2.27E–03	3.83E–05	6.4	0
2.4	Fe(II)	0.01	0	N	3.02E–03	8.71E–04	bd	–	6.9	0
2.4	Fe(II)	0.01	5	N	3.77E–04	4.43E–05	3.30E–03	7.48E–04	6.8	0.1
2.4	Fe(II)	0.01	14	N	3.62E–04	2.21E–05	4.78E–03	5.39E–04	6.7	0
1.9	Fe(II)	3.5	0	N	3.7	8.37E–02	nd	–	5.5	0.2
1.9	Fe(II)	3.5	5	N	3.6	1.45E–01	nd	–	5.1	0
1.9	Fe(II)	3.5	14	N	3.7	3.21E–01	4.70E–03	6.64E–03	5.1	0
2.4	Fe(II)	2.1	0	N	1.8	1.60E–01	nd	–	5.9	0.1
2.4	Fe(II)	2.1	5	N	2.1	7.87E–02	nd	–	5.8	0
2.4	Fe(II)	2.1	14	N	1.8	2.12E–01	3.41E–01	3.64E–01	6	0
1.9	S(II)	0.05	0	N	8.00E–01	1.53E–02	nd	–	6.5	0.1
1.9	S(II)	0.05	5	N	9.25E–02	4.22E–02	1.88E–02	1.67E–02	6.4	0.1
1.9	S(II)	0.05	14	N	5.53E–02	5.23E–03	5.16E–03	1.53E–03	6.4	0
2.4	S(II)	0.05	0	N	2.91E–01	5.86E–03	7.67E–02	4.43E–03	7	0.1
2.4	S(II)	0.05	5	N	1.70E–03	3.83E–03	1.78E–02	7.45E–03	7	0
2.4	S(II)	0.05	14	N	1.82E–02	4.22E–03	1.71E–02	2.98E–03	6.9	0.1
1.9	S(II)	0.6	0	N	1.61E–02	2.65E–03	1.35E–03	3.10E–04	6.6	0.1
1.9	S(II)	0.6	5	N	1.23E–02	7.51E–04	1.46E–03	3.76E–04	6.8	0
1.9	S(II)	0.6	14	N	1.28E–02	6.02E–03	2.07E–03	3.66E–04	6.9	0.1
2.4	S(II)	0.6	0	N	nd	–	nd	–	7.8	0.1
2.4	S(II)	0.6	5	N	1.08E–03	3.31E–04	3.11E–03	5.20E–04	8.1	0.1
2.4	S(II)	0.6	14	N	9.09E–04	2.89E–04	4.98E–03	5.03E–04	8.2	0
2.5	Fe(II)	3.8	0	Y	3.30	2.99E–01	–7.01E–02	4.98E–02	–	–
2.5	Fe(II)	3.8	5	Y	4.20	3.59E–01	nd	–	–	–
2.5	Fe(II)	3.8	14	Y	3.10	2.97E–01	nd	–	–	–
3.5	Fe(II)	2.3	0	Y	nd	–	2.15	–	–	–
3.5	Fe(II)	2.3	5	Y	2.40	–	nd	–	–	–
3.5	Fe(II)	2.3	14	Y	1.80	–	nd	–	–	–
2.5	S(II)	0.05	0	Y	1.74E–03	1.11E–03	2.68E–03	5.91E–04	–	–
2.5	S(II)	0.05	5	Y	2.83E–04	4.00E–04	1.87E–04	8.02E–05	–	–
2.5	S(II)	0.05	14	Y	nd	–	2.27E–03	7.44E–04	–	–
3.5	S(II)	0.05	0	Y	1.14E–02	–	1.04E–04	–	–	–
3.5	S(II)	0.05	5	Y	nd	–	1.11E–04	–	–	–
3.5	S(II)	0.05	14	Y	nd	–	2.71E–03	–	–	–
2.5	S(II)	0.6	0	Y	7.38E–02	7.85E–03	3.30E–02	2.88E–03	–	–
2.5	S(II)	0.6	5	Y	9.17E–02	4.07E–02	nd	–	–	–
2.5	S(II)	0.6	14	Y	3.56E–02	3.77E–02	8.45E–04	9.48E–04	–	–
3.5	S(II)	0.6	0	Y	1.14E–01	–	3.37E–02	–	–	–
3.5	S(II)	0.6	5	Y	1.63E–01	–	8.73E–04	–	–	–
3.5	S(II)	0.6	14	Y	4.90E–02	–	nd	–	–	–

analysis of DOM can provide information regarding average molecular properties, DOM most likely consists of multiple chemical domains, each largely homogenous and distinct. Moreover, it is interesting that the process of precipitation and complexation with Fe alone appears sufficient to physically and chemically separate these domains. This implies that these chemically distinct groups are relatively loosely associated with each other.

The propensity of polysaccharide C to associate with Fe is supportive of the bulk fractionation observed by Eusterhues et al. (2011). The varying electronic environment of the Fe atoms with the binding strength of the DOM implies that isolated or very small clusters of Fe centers are in direct molecular association with the carboxyl or hydroxyl functional groups. It has been observed that the size of the crystalline regions of precipitated Fe (hydr)oxide material can be diminished in the presence of OM (Cismasu et al., 2011) and our results appear to represent an extreme case of this phenomenon, possibly due to higher C:Fe values.

The association of distinct OM functional groups with Fe in our STXM data is consistent with the proposed mechanisms of coprecipitation of OM, which favors the complexation of more aromatic, higher molecular weight (MW) material associated with a higher proportion of carboxylic acids (Edwards and Cresser, 1983; Gu, 1995; Sharp et al., 2006). The apparent exclusion of the amide and aromatic rich OM is surprising given that, according to SUVA

measurements in this and previous studies, aromatic OM is preferentially removed from solution through flocculation (Dennett et al., 1996). However, it is possible that the more hydrophobic aromatic OM is prone to partition out of solution phase to form micellar associations within the floc or requires only a very small amount of associated Fe for the purposes of charge balance in order to induce precipitation. This is consistent with the view that the first additions of Fe preferentially remove highly aromatic material, while larger quantities of Fe are needed to remove the more oxidized material (Matilainen et al., 2011). This leads to the situation where the majority of the Fe is associated with the more oxidized carboxylic or O-alkyl containing OM. Alternatively, as seen in Region 2 of the floc, it is possible that the floc structure provides microenvironments for preferential concentration of certain other types of OM, for example high MW proteins that do not directly involve complexation with Fe. In contrast, the carbon chemistry of the particle in Fig. 2b was highly uniform, with all regions returning spectra similar to that in Fig. 2d.

3.2. Floc reactivity

3.2.1. DOC concentration and SUVA characteristics vs. time

Although pH was adjusted initially to 6.5, upon addition of Fe(II) the pH of the unbuffered treatments dropped to 4.6–5.4. In con-

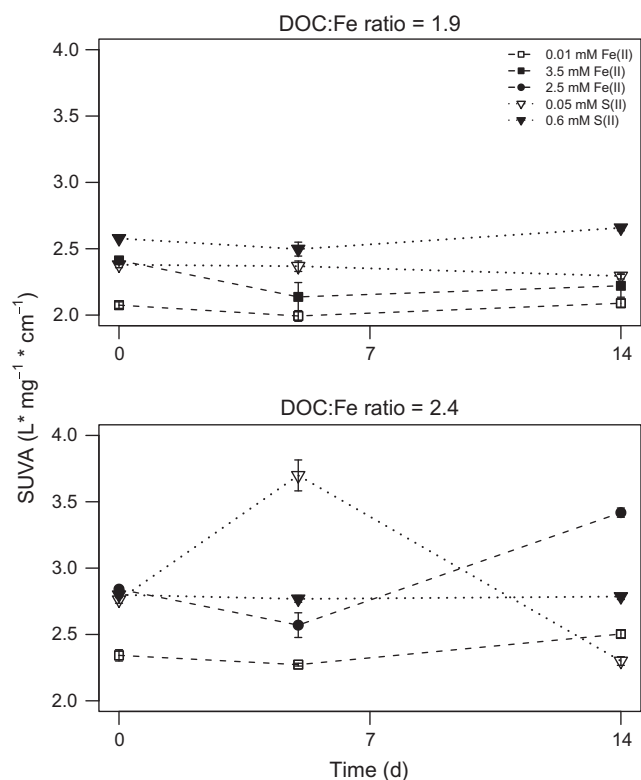


Fig. 3. SUVA values of solutions for unbuffered treatments with OM present receiving different reductant concentration. Top panel depicts treatments with higher Fe coagulant dose, while bottom panel represents treatments with lower Fe coagulant dose. DOC: Fe ratio is for values within the floc. Points depict means, vertical lines show standard deviation of the mean ($n = 3$).

trast, addition of S(-II) increased pH to 6.2–8.2 (Table 3, Supplementary information). This change caused some release or uptake of DOC on day 0 for the treatment receiving the higher doses of S(-II) and Fe(II), respectively (Fig. 2). However, <10% overall of the original DOC incorporated into the floc was released as a result of the initial pH change. The only exception was for the higher S(-II) addition which increased the pH to 8.2, releasing up to 50% of the floc C. Over the 14 day incubation period, there was no evidence of further release of DOC from any of the unbuffered treatments; change in DOC concentration was $\pm 10\%$.

The shift from higher SUVA values in the original solution to lower values following coagulation indicates preferential removal of the aromatic, high MW DOM fraction from solution (Fig. 3; Blough and del Vecchio, 2002; Weishaar et al., 2003). Like the DOC concentration, there was minimal change in SUVA values ($\pm 10\%$) for the unbuffered treatments over time, with the exception of the lower S(-II) and Fe(II) treatments, which increased on day 5 and 14, respectively.

These results for both DOC concentration and SUVA values indicate the fraction of DOC removed through coagulation remained within the floc over time in spite of the addition of reductant and resulting changes in Fe crystallization (Section 3.3). There was also no evidence of exchange between the more aromatic (higher SUVA) DOM sequestered by the floc and the less aromatic (lower SUVA) DOM in solution.

3.2.2. Effect of Fe concentration

Total Fe concentration in the low Fe(II) treatments (0.01 mM) was below raw water solution concentration for the unbuffered treatments (Table 3) and below detection (0.36 mM) for all unbuffered treatments containing no DOM, except for the day 0 treat-

ments receiving a coagulant addition of 2.2 mmol l^{-1} Fe (Supplementary information). For both the buffered and unbuffered treatments receiving equimolar addition of Fe(II) and Fe(III) in the coagulant [2.3–3.8 mM Fe(II)], some Fe(II) – up to 20% – was initially lost from solution on day 0. There was a general increase in total solution Fe on day 5 followed by a decrease on day 14 (Table 3). Fe(III) release from both buffered and unbuffered treatments coprecipitated with DOM was close to zero (Table 3).

The decrease in solution Fe(II) in the treatments receiving equimolar Fe(II) is most likely due to the association of the reductant with the surface of Fe (hydr)oxide centers within the floc or unsatisfied complexation sites within the OM. The release of Fe(II) towards the middle of the incubation, especially for samples with no OM, most (Pedersen et al., 2005) likely resulted from the reductive dissolution of floc by added Fe(II) (Wehrli et al., 1989). Fe(II)-catalyzed dissolution of Fe(III) has been found to occur but it is interesting to note that the release of Fe(III) in treatments lacking DOM was higher than those coprecipitated with DOM (Supplementary table), as this indicates DOM may reduce the reactivity of the Fe (hydr)oxide. As discussed in Section 3.1, carboxylic acids play a large role in the complexation during coprecipitation and coagulation. This strong, inner-sphere complexation of carboxylic groups with the Fe (hydr)oxide group may have interfered with the Fe(II) mediated dissolution of Fe(III).

3.2.3. Effect of sulfide concentration

In treatments that received a lower S(-II) concentration (0.05 mM), small amounts of Fe(II) were present in solution immediately after S(-II) addition, but gradually decreased to or below detection limit in most treatments (Table 3). Little to no dissolution of Fe(II) (<0.4% of floc) occurred with addition of higher S(-II) (0.6 mM) in spite of visual darkening indicative of FeS formation. Previous studies that used ferrihydrite and poorly crystalline iron oxides to remove sulfide from water have also found release of dissolved Fe to be negligible (Poulton, 2003).

S(-II) is known to react with Fe oxide species through an inner-sphere complexation and subsequent electron transfer to the Fe(III) species (Afonso and Stumm, 1992), so the initial release of Fe for the lower S(-II) treatments is most likely due to reductive dissolution of the floc surface by the added S(-II). The Fe(II) released initially may have reacted with unreduced floc Fe or with the additional S(-II) in solution to form a secondary solid Fe(II)-sulfide species (Poulton, 2003; Slowey and Brown, 2007).

A higher concentration of S(-II) has been found to result in enhanced rates of Fe-sulfide precipitate formation (Pyzik and Sommer, 1981), which may be why Fe release was lower for this treatment than treatments with a lower concentration of S(-II). However, no iron sulfide minerals were detected via XRD analysis (Section 3.3) although this could be due to the limited sensitivity of XRD to small grain size or short-range order material. In spite of these obvious changes in Fe chemistry there was, however, no significant release of DOM to solution.

3.3. Floc crystallinity

X-ray diffraction was used to determine the formation of more crystalline Fe oxides and sulfides. There was no apparent development of crystallinity nor even formation of ferrihydrite-like characteristics in treatments that did not receive Fe(II) or S(-II) over the 14 day incubation period (see Fig. in Supplementary information). This implies that the presence of an electron donor was required for crystallization of Fe(III) under experimental conditions. All DOM-free treatments that received either Fe(II) or S(-II) formed goethite peaks by day 5 and an unidentifiable peak for the treatment receiving the lower dose of S(-II) (Figs. 4 and 5). In contrast, there was no apparent crystallization for samples containing Fe

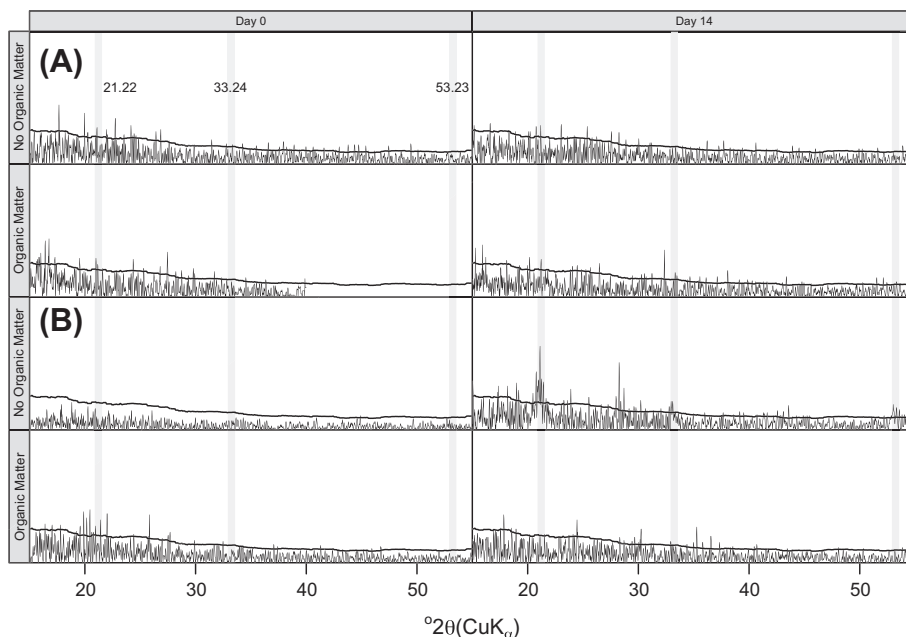


Fig. 4. X-ray diffraction curve for unbuffered treatments receiving Fe(II). (A) Spectra for treatments receiving lower concentration of Fe(II) (0.01 mM). Slide for treatment containing OM was only run up to $40^{\circ} 2\theta$. (B) Spectra for treatments receiving higher concentration of Fe(II) (3.5 mM). Black line depicts detection limit calculated as a 97.5% confidence interval around angle dependent mean of a day 0 control (no reductant) floc containing OM. Gray vertical lines depict location of goethite peaks. Numeric values depict location of peaks.

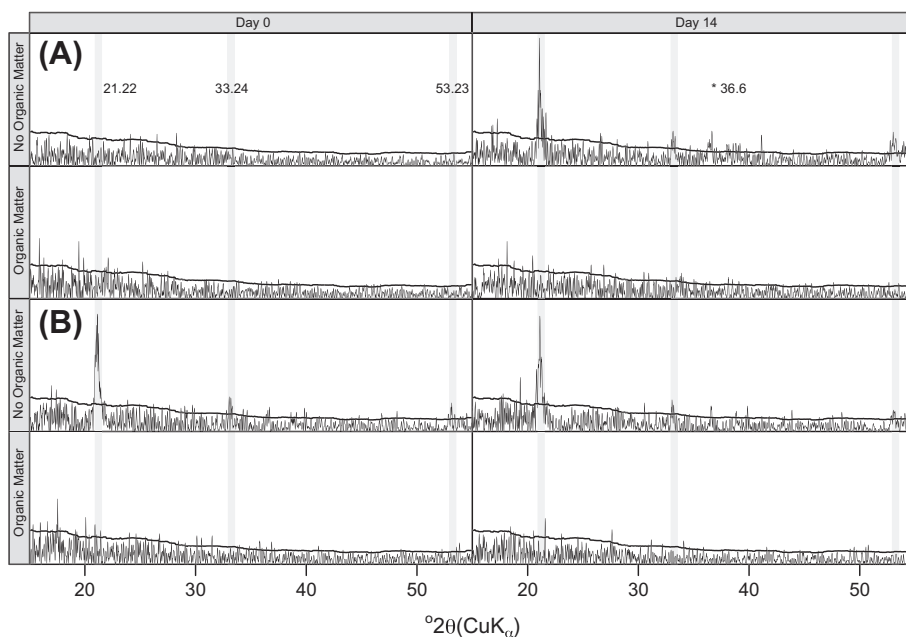


Fig. 5. X-ray diffraction curve for buffered treatments receiving S(-II) amendments. (A) Spectra for lower concentration of sulfide (0.05 mM); (B) spectra for higher amendment (0.6 mM). Black line depicts detection limit calculated as 99.9% confidence interval around angle dependent mean of a day 0 control (no reductant) floc containing OM. Gray vertical lines depict location of goethite peaks. Starred (*) value in second panel depicts unidentified peak.

coprecipitated with DOM, even by day 14 for both unbuffered and buffered treatments. This indicates that coprecipitated OM inhibited reductive crystallization of the Fe (hydr)oxides during the 14 day period. As there was no obvious difference in crystallization character between the unbuffered and buffered XRD spectra, the Figs. and the discussion below reflect data from the buffered treatments.

Higher addition of Fe(II) in the DOM-free treatments resulted in formation of mainly goethite peaks by day 5 (Fig. 4). Although goethite is a common species formed upon reductive transformation

of poorly crystalline Fe (hydr)oxides (Cornell and Schneider, 1989; Kukkadapu et al., 2003), the lack of magnetite formation is in contrast to previous findings (Hansel et al., 2005; Yang et al., 2010). The formation of minerals on day 5 coincides with the increase in soluble Fe(II) in solution, supporting re-crystallization to lower surface area mineral phases with lower Fe(II) adsorption capacity (Wehrli et al., 1989).

Treatments with no DOM that received the lower S(-II) amendment showed increased crystallinity by day 5, with more

prominent goethite peaks (Fig. 5) vs. both the high Fe(II) and high S(-II) treatments. On the other hand, treatment in the absence of DOM amended with the higher concentration of S(-II) crystallized immediately, forming goethite, and eventually akageneite (Fig. 5).

As S(-II) is a stronger reductant for Fe(III) than Fe(II), the rate of electron exchange and subsequent formation of secondary minerals is most likely higher for S(-II), resulting in an enhanced rate of mineral formation than for the Fe(II) treatments. The higher S(-II) treatments may have immediately formed poorly crystalline iron-sulfide complexes with the floc, as indicated by the darkening of the samples upon S(-II) addition. The formation of iron sulfide species may have competed with other mineral formation, resulting in less prominent peaks than those for the low S(-II) addition. While no FeS minerals were identified in the XRD analysis, this does not preclude the presence of small particle size, poorly ordered FeS, such as Fe monosulfide, common in wetland soils of the region (Maynard et al., 2011). In the low S(-II) treatments, there may have been more available Fe(II) in solution due to the lower concentration of S(-II), which is important for the amount and species of secondary minerals formed (Tufano et al., 2009).

4. Summary and implications

The presence of coprecipitated OM strongly inhibited the reductive crystallization of Fe (hydr)oxide materials. The DOM-Fe (hydr)oxide interaction produced a stable floc material that did not release DOM back into solution regardless of pH, Fe:DOM ratio and type of reductant added. The results indicate the potential usefulness of Fe-DOM complexation in the long term removal of DOM from wetland environments as well as the importance of Fe-DOM complexes for OM stabilization in soil, even under reducing conditions. In addition, they illustrate that, although coprecipitated Fe phases decreased structural order, they may not in fact be more reactive.

The mechanism of coagulation and coprecipitation may result in different bond strength and molecular conformations from adsorption of OM to pre-formed Fe (hydr)oxides. Coprecipitation may result in reconfirmation of the OM around the positively charged Fe, resulting in micellar interactions and tighter coiling of DOM (Jung et al., 2005; Siéliéchi et al., 2008). This reformation, in addition to the strong inner sphere complexation of carboxylic groups with the Fe, is most likely behind inhibition of reductive transformation of the Fe mineral. Competition between the reductant and the OM and Fe (hydr)oxide would limit dissolution and re-crystallization of the floc. In support, O'Loughlin et al. (2010) found that complex natural OM inhibited reductive dissolution of lepidocrocite and attributed the phenomenon to the binding of competing anions that formed inner sphere complexes, such as OM, that were not easily displaced by biotic and abiotic reducing agents.

The use of low MW algal and polysaccharide-based C compounds in past coprecipitation studies may have resulted in different bonding mechanisms between the OM and Fe and may not represent what occurs naturally; this may explain why these studies concluded that OM induced Fe reduction. Some of these coprecipitation studies were also conducted with OM solutions under initially acidic conditions, ranging from pH 2–3 (Mikutta et al., 2008; Jones et al., 2009). Under acidic conditions, Fe is more hydrolyzed and the structure of OM may be different from more neutral conditions, which may affect the bond strength and reactivity of the final product.

The study was conducted to assess the feasibility of retaining residual floc resulting from the coagulation of DOM with Fe-based coagulants in constructed wetlands. The application of the method is underway in the Sacramento-San Joaquin Delta and studies are

being conducted to determine the stability of the floc under various wetland conditions. There is currently a dearth of knowledge regarding the long term stability of such Fe-organo floc under different redox environment conditions. Results from the study indicate that the method may be feasible under laboratory conditions. Future studies should employ a biological component to determine effects of microbial activity on floc reactivity, more varied C to Fe ratio values, and include field-based studies to address various toxicity issues as well as isotopic experiments using labeled Fe to trace the fate of Fe (hydr)oxides under varying conditions.

Acknowledgements

The overlying project for this work (Low Intensity Chemical Dosing) was initiated by R. Fujii and P. Bachand. Research was made possible from funding by the California Department of Water Resource (Agreement #v4600003886) and matching funds provided by the US Geological Survey. Partial funding was supplied by the US Department of Energy, Office of Biological and Environmental Sciences via the LBNL Earth Sciences Sustainable Systems Science focus area under contract DE-AC02-05CH11231. Access to beamline 5.3.2.2. was provided by the ALS which is supported by the Director, Office of Science, Office of Basic Energy Sciences of the U.S. Department of Energy under the same contract. We would like to thank R. Dahlgren and two anonymous reviewers for insightful comments. We would also like to thank T. Doane and J. Nugent for assistance with laboratory analysis and R. Soutard for XRD expertise. Use of trade names is for identification purposes and does not imply endorsement by the U.S. Government.

Appendix A. Supplementary material

Supplementary data associated with this article can be found, in the online version, at <http://dx.doi.org/10.1016/j.orggeochem.2012.04.005>.

Associate Editor—L. Schwark

References

- Afonso, M.D., Stumm, W., 1992. Reductive dissolution of iron (III) (Hydr)oxides by hydrogen-sulfide. *Langmuir* 8, 1671–1675.
- Armbruster, M.K., Schimmelpfennig, B., Plaschke, M., Rothe, J., Denecke, M.A., Klenze, R., 2009. Metal-ion complexation effects in C 1s-NEXAFS spectra of carboxylic acids – evidence by quantum chemical calculations. *Journal of Electron Spectroscopy and Related Phenomena* 169, 51–56.
- Bachand, P.A.M., Richardson, C.J., Vaithyanathan, P., 2000. Phase II Low Intensity Chemical Dosing (LICD): Development of Management Practices. Final report submitted to Florida Department of Environmental Protection in fulfillment of Contract No. WM720.
- Bachand, P., Trejo-Gaytan, J., Darby, J., Reuter, J., 2006. Final Report: Small-Scale Studies on Low Intensity Chemical Dosing (LICD) for Treatment of Highway Runoff. Submitted to CALTRANS (California Department of Transportation) by University of California Davis.
- Benner, S.G., Hansel, C.M., Wielinga, B.W., Barber, T.M., Fendorf, S., 2002. Reductive dissolution and biomineralization of iron hydroxide under dynamic flow conditions. *Environmental Science & Technology* 36, 1705–1711.
- Blodau, C., Roehm, C.L., Moore, T.R., 2002. Iron, sulfur, and dissolved carbon dynamics in a northern peatland. *Archiv für Hydrobiologie* 154, 561–583.
- Blough, N., del Vecchio, R., 2002. Chromophoric DOM in the coastal environment. In: Hansell, D., Carlson, A. (Eds.), *Biogeochemistry of Marine Dissolved Organic Matter*. Academic Press, San Diego, CA, pp. 509–546.
- Chan, C.S., Fakra, S.C., Edwards, D.C., Emerson, D., Banfield, J.F., 2009. Iron oxyhydroxide mineralization on microbial extracellular polysaccharides. *Geochimica et Cosmochimica Acta* 73, 3807–3818.
- Choi, J.H., Park, S.S., Jaffe, P.R., 2006. Simulating the dynamics of sulfur species and zinc in wetland sediments. *Ecological Modelling* 199, 315–323.
- Christl, I., Kretschmar, R., 2007. C-1s NEXAFS spectroscopy reveals chemical fractionation of humic acid by cation-induced coagulation. *Environmental Science & Technology* 41, 1915–1920.
- Cismasu, A.C., Michel, F.M., Tcaciuc, A.P., Tyliczszak, T., Brown, J., Gordon, E., Brown Jr., G.E., 2011. Composition and structural aspects of naturally occurring ferrihydrite. *Comptes Rendus Geoscience* 343, 210–218.

- Cornell, R.M., Schneider, W., 1989. Formation of goethite from ferrihydrite at physiological pH under the influence of cysteine. *Polyhedron* 8, 149–155.
- Cornell, R.M., Schwertmann, U., 1979. Influence of organic-anions on the crystallization of ferrihydrite. *Clays and Clay Minerals* 27, 402–410.
- Dempsey, B.A., Ganho, R.M., Omelia, C.R., 1984. The coagulation of humic substances by means of aluminum salts. *American Water Works Association Journal* 76, 141–150.
- Dennett, K.E., Amiratharajah, A., Moran, T.F., Gould, J.P., 1996. Coagulation: its effect on organic matter. *American Water Works Association Journal* 88, 129–142.
- Dentel, S.K., Kingery, K.M., 1989. Using streaming current detectors in water treatment. *American Water Works Association Journal* 81, 85–94.
- Deverel, S.J., Leighton, D.A., Finlay, M.R., 2007. Processes Affecting Agricultural Drainwater Quality and Organic Carbon Loads in California's Sacramento-San Joaquin Delta. Quality.
- Doane, T.A., Horwath, W.R., 2010. Eliminating interference from iron (III) for ultraviolet absorbance measurements of dissolved organic matter. *Chemosphere* 78, 1409–1415.
- Downing, B.D., Bergamaschi, B.A., Evans, D.G., Boss, E., 2008. Assessing contribution of DOC from sediments to a drinking-water reservoir using optical profiling. *Lake and Reservoir Management* 24, 381–391.
- Edwards, A.C., Cresser, M.S., 1983. An improved, automated xylenol orange method for the colorimetric determination of aluminum. *Talanta* 30, 702–704.
- Emerson, D., Weiss, J., 2004. Bacterial iron oxidation in circumneutral freshwater habitats: Findings from the field and the laboratory. *Geomicrobiology Journal* 21, 405–414.
- Eusterhues, K., Wagner, F.E., Häusler, W., Hanzlik, M., Knicker, H., Totsche, K.U., Kögel-Knabner, I., Schwertmann, U., 2008. Characterization of ferrihydrite-soil organic matter coprecipitates by X-ray diffraction and Mössbauer spectroscopy. *Environmental Science & Technology* 42, 7891–7897.
- Eusterhues, K., Rennert, T., Knicker, H., Kögel-Knabner, I., Totsche, K.U., Schwertmann, U., 2011. Fractionation of organic matter due to reaction with ferrihydrite: coprecipitation versus adsorption. *Environmental Science & Technology* 45, 527–533.
- Fuller, C.C., Davis, J.A., Waychunas, G.A., 1993. Surface-chemistry of ferrihydrite. 2. Kinetics of arsenate adsorption and coprecipitation. *Geochimica et Cosmochimica Acta* 57, 2271–2282.
- Glasauer, S., Weidler, P.G., Langley, S., Beveridge, T.J., 2003. Controls on Fe reduction and mineral formation by a subsurface bacterium. *Geochimica et Cosmochimica Acta* 67, 1277–1288.
- Gu, B., 1995. Adsorption and desorption of different organic matter fractions on iron oxide. *Geochimica et Cosmochimica Acta* 59, 219–229.
- Hansel, C.M., Benner, S.G., Fendorf, S., 2005. Competing Fe(II)-induced mineralization pathways of ferrihydrite. *Environmental Science & Technology* 39, 7147–7153.
- Henneberry, Y.K., Kraus, T.E.C., Fleck, J.A., Krabbenhoft, D.P., Bachand, P.M., Horwath, W.R., 2011. Removal of inorganic mercury and methylmercury from surface waters following coagulation of dissolved organic matter with metal-based salts. *Science of the Total Environment* 409, 631–637.
- Hiemstra, T., Van Riemsdijk, W.H., 2009. A surface structural model for ferrihydrite I: sites related to primary charge, molar mass, and mass density. *Geochimica et Cosmochimica Acta* 73, 4423–4436.
- Hocking, R.K., DeBeer George, S., Raymond, K.N., Hodgson, K.O., Hedman, B., Solomon, E.I., 2010. Fe L-edge X-ray absorption spectroscopy determination of differential orbital covalency of siderophore model compounds: electronic structure contributions to high stability constants. *Journal of the American Chemical Society* 132, 4006–4015.
- Jones, A.M., Pham, A.N., Collins, R.N., Waite, T.D., 2009. Dissociation kinetics of Fe(III)- and Al(III)-natural organic matter complexes at pH 6.0 and 8.0 and 25 °C. *Geochimica et Cosmochimica Acta* 73, 2875–2887.
- Jung, a-V.V., Chanudet, V., Ghanbaja, J., Lartiges, B.S., Bersillon, J.-L.L., 2005. Coagulation of humic substances and dissolved organic matter with a ferric salt: an electron energy loss spectroscopy investigation. *Water Research* 39, 3849–3862.
- Knorr, K.H., Lischheid, G., Blodau, C., 2009. Dynamics of redox processes in a minerotrophic fen exposed to a water table manipulation. *Geoderma* 153, 379–392.
- Kraus, T.E.C., Bergamaschi, B.A., Hernes, P.J., Spencer, R.G.M., Stepanauskas, R., Kendall, C., Losee, R.F., Fujii, R., 2008. Assessing the contribution of wetlands and subsided islands to dissolved organic matter and disinfection byproduct precursors in the Sacramento-San Joaquin River Delta: a geochemical approach. *Organic Geochemistry* 39, 1302–1318.
- Kukkadapu, R.K., Zachara, J.M., Fredrickson, J.K., Smith, S.C., Dohnalkova, A.C., Russell, C.K., 2003. Transformation of 2-line ferrihydrite to 6-line ferrihydrite under oxic and anoxic conditions. *American Mineralogist* 88, 1903–1914.
- Larsen, O., Postma, D., 2001. Kinetics of reductive bulk dissolution of lepidocrocite, ferrihydrite, and goethite. *Geochimica et Cosmochimica Acta* 65, 1367–1379.
- Matilainen, A., Gjessing, E.T., Lahtinen, T., Hed, L., Bhatnagar, A., Sillanpää, M., 2011. An overview of the methods used in the characterisation of natural organic matter (NOM) in relation to drinking water treatment. *Chemosphere* 83, 1431–1442.
- Maynard, J.J., O'Geen, A.T., Dahlgren, R.A., 2011. Sulfide induced mobilization of wetland phosphorus depends strongly on redox and iron geochemistry. *Soil Science Society of America Journal* 75.
- Mikutta, C., 2011. X-ray absorption spectroscopy study on the effect of hydroxybenzoic acids on the formation and structure of ferrihydrite. *Geochimica et Cosmochimica Acta* 75, 5122–5139.
- Mikutta, C., Mikutta, R., Bonneville, S., Wagner, F., Voegelin, A., Christl, I., Kretzschmar, R., 2008. Synthetic coprecipitates of exopolysaccharides and ferrihydrite. Part 1: Characterization. *Geochimica et Cosmochimica Acta* 72, 3292.
- Mourad, D., 2003. Investigating the use of Coagulation Seasonally to Reduce DOC and DBP Precursor Loads from Subsidized Islands in the Sacramento-San Joaquin Delta. M.Sc. Thesis. University of California, Davis.
- O'Loughlin, E.J., Gorski, C.A., Scherer, M.M., Boyanov, M.I., Kemner, K.M., Loughlin, E.J.O., 2010. Effects of oxyanions, natural organic matter, and bacterial cell numbers on the bioreduction of lepidocrocite (gamma-FeOOH) and the formation of secondary mineralization products. *Environmental Science & Technology* 44, 4570–4576.
- Pedersen, H., Postma, D., Jakobsen, R., Larsen, O., 2005. Fast transformation of iron oxyhydroxides by the catalytic action of aqueous Fe(II). *Geochimica et Cosmochimica Acta* 69, 3967–3977.
- Pokrovsky, O.S., Schott, J., 2002. Iron colloids/organic matter associated transport of major and trace elements in small boreal rivers and their estuaries (NW Russia). *Chemical Geology* 190, 141–179.
- Poulton, S.W., 2003. Sulfide oxidation and iron dissolution kinetics during the reaction of dissolved sulfide with ferrihydrite. *Chemical Geology* 202, 79–94.
- Pullin, M.J., Cabaniss, S.E., 2001. Colorimetric flow-injection analysis of dissolved iron in high DOC waters. *Water Research* 35, 363–372.
- Pyzik, A.J., Sommer, S.E., 1981. Sedimentary iron monosulfides-kinetics and mechanism of formation. *Geochimica et Cosmochimica Acta* 45, 687–698.
- Schumacher, M., Christl, I., Vogt, R.D., Barmettler, K., Jacobsen, C., Kretzschmar, R., 2006. Chemical composition of aquatic dissolved organic matter in five boreal forest catchments sampled in spring and fall seasons. *Biogeochemistry* 80, 263–275.
- Schwertmann, U., Murad, E., 1983. Effect of pH on the formation of goethite and hematite from ferrihydrite. *Clays and Clay Minerals* 31, 277–284.
- Sharp, E.L., Parsons, S.A., Jefferson, B., 2006. Seasonal variations in natural organic matter and its impact on coagulation in water treatment. *Science of the Total Environment* 363, 183–194.
- Sholkovitz, E.R., 1976. Flocculation of dissolved organic and inorganic matter during mixing of river water and seawater. *Geochimica et Cosmochimica Acta* 40, 831–845.
- Siéliéchi, J.-M., Lartiges, B.S., Kayem, G.J., Hupont, S., Frochot, C., Thieme, J., Ghanbaja, J., Espinose, d., de la Caillerie, J.B., Barrès, O., Kamga, R., Levitz, P., Michot, L.J., Sieliéchi, J.M., de la Caillerie, J.B.D., Barres, O., 2008. Changes in humic acid conformation during coagulation with ferric chloride: implications for drinking water treatment. *Water Research* 42, 2111–2123.
- Slowey Jr., A.J., Brown, G.E., 2007. Transformations of mercury, iron, and sulfur during the reductive dissolution of iron oxyhydroxide by sulfide. *Geochimica et Cosmochimica Acta* 71, 877–894.
- Tufano, K.J., Benner, S.G., Mayer, K.U., Marcus, M.A., Nico, P.S., Fendorf, S., 2009. Aggregate-scale heterogeneity in iron (hydr)oxide reductive transformations. *Vadose Zone Journal* 8, 1004–1012.
- Tugel, A.J., 1993. Soil survey of Sacramento County, California. USDA Soil Conservation Service in cooperation with Regents of the University of California Agricultural Experimental Station, Washington, DC.
- Viollier, E., Inglett, P.W., Hunter, K., Roychoudhury, A.N., Van Cappellen, P., 2000. The ferrozine method revisited: Fe(II)/Fe(III) determination in natural waters. *Applied Geochemistry* 15, 785–790.
- von Luetzow, M., Kögel-Knabner, I., Ekschmitt, K., Matzner, E., Guggenberger, G., Marschner, B., Flessa, H., 2006. Stabilization of organic matter in temperate soils: mechanisms and their relevance under different soil conditions – a review. *European Journal of Soil Science* 57, 426–445.
- Warwick, T., Ade, H., Kilcoyne, D., Kritscher, M., Tyliczcak, T., Fakra, S., Hitchcock, A., Hitchcock, P., Padmore, H., 2002. A new bend-magnet beamline for scanning transmission X-ray microscopy at the Advanced Light Source. *Journal of Synchrotron Radiation* 9, 254–257.
- Wehrli, B., Sulzberger, B., Stumm, W., 1989. Redox processes catalyzed by hydrous oxide surfaces. *Chemical Geology* 78, 167–179.
- Weishaar, J.L., Aiken, G.R., Bergamaschi, B.A., Fram, M.S., Fujii, R., Mopper, K., 2003. Evaluation of specific ultraviolet absorbance as an indicator of the chemical composition and reactivity of dissolved organic carbon. *Environmental Science & Technology* 37, 4702–4708.
- Weiss, J.V., Emerson, D., Megonigal, J.P., 2004. Geochemical control of microbial Fe(III) reduction potential in wetlands: comparison of the rhizosphere to non-rhizosphere soil. *FEMS Microbiology Ecology* 48, 89–100.
- Yang, L., Steefel, C.L., Marcus, M.A., Bargar, J.R., 2010. Kinetics of Fe(II)-catalyzed transformation of 6-line ferrihydrite under anaerobic flow conditions. *Environmental Science & Technology* 44, 5469–5475.